Cauchy integrals for computational solutions of master equations

S. MacNamara[1]

(Received 26 February 2015; revised 21 September 2015)

Abstract

Cauchy contour integrals are demonstrated to be effective in computationally solving master equations. A fractional generalization of a bimolecular master equation is one interesting application.

Contents

1   Introduction

A celebrated result of complex analysis is the *Cauchy integral formula*:

$$f(a) = \frac{1}{2\pi i} \int_\Gamma f(z)(z-a)^{-1} dz \,.$$

Here the function f is analytic on a simple domain $D \subset \mathbb{C}$ containing the smooth contour $\Gamma \subset D$, which winds once counter-clockwise around the point a [32]. For the Laplace transform of f, $F(s) \equiv \mathcal{L}\{f\} = \int_0^\infty e^{-st} f(t) dt$, the inverse Laplace transform

$$\mathcal{L}^{-1}\{F\}(t) = \frac{1}{2\pi i} \int_{\gamma-i\infty}^{\gamma+i\infty} e^{st} F(s) ds \,,$$
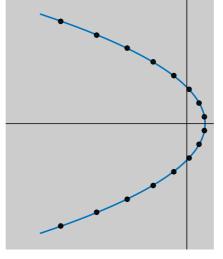
comes via Cauchy's formula and is known as the Bromwich integral. The contour in this case is a vertical line parallel to the imaginary axis with real part γ to the right of all singularities of F. By Cauchy's integral theorem, the integral is path independent so there is freedom to choose a different contour Γ if that is more convenient. The inverse Laplace transform and all examples to come in this article involve integrands with a factor e^z so the integrand is exponentially small in regions where $\operatorname{Re}(z) < 0$. This observation has inspired numerical methods based on contours that pass through the left-half plane to take advantage of exponentially small integrands. Such Hankel contours resemble a sideways parabola (Figure 1) that encloses the negative real axis $(-\infty, 0]$, winding around the origin once.

Truncating the infinite contour Γ to only a finite part, say $\operatorname{Re}(z) > -50$, introduces only an exponentially small error because of the e^z factor. For

Figure 1: The parabolic contour Γ to compute the Cauchy integral (2).

$\theta \in \mathbb{R}$ and $N = 2^4$, this article uses a parabola (Figure 1) optimised by Weideman and Trefethen [40, 43]:

$$z(\theta) = N(0.1309 - 0.1194\,\theta^2 + 0.25i\,\theta)\,. \tag{1}$$

John Butcher [4] and Alan Talbot [37] were amongst the first to suggest using the Cauchy formula numerically in this way to find inverse Laplace transforms.

The Cauchy integral formula generalizes to define a matrix function [13]: $2\pi i\, f(A) = \int_\Gamma f(z)(zI - A)^{-1}dz$, (where I is the identity matrix). Indeed, it generalizes to operator settings [17, 8] but we consider only the case of a finite and bounded matrix A with distinct real eigenvalues that are negative or zero: $\lambda_i \leqslant 0$. For example, put $f(z) = e^z$ to see the matrix exponential e^A as the inverse Laplace transform of the *resolvent* $(zI - A)^{-1}$. Multiply both sides by a vector $\boldsymbol{v}$ because (without explicitly forming a full matrix such as $f(A)$) we directly compute $f(A)\boldsymbol{v}$ as the action of a matrix function on a

vector:
$$f(A)\boldsymbol{v} = \frac{1}{2\pi i} \int_\Gamma f(z)(zI - A)^{-1}\boldsymbol{v}\, dz \,. \tag{2}$$

Evaluating the integral involves solving shifted linear systems at nodes (dots in Figure 1) $z_k = z(\theta_k)$ on Γ in (1), in a quadrature approximation to (2):

$$f(A)\boldsymbol{v} \approx \sum_{k=1}^{N} w_k \boldsymbol{u_k} \quad \text{where} \quad (z_k I - A)\boldsymbol{u_k} = \boldsymbol{v} \,. \tag{3}$$

Experiments here use the trapezoidal-like methods of Weideman and Trefethen [43] and all involve a factor e^{z_k}. Weideman and Trefethen [43] discuss more details, such as nodes z_k and the quadrature weights $w_k(z_k)$.

Via (3) we compute two functions: an exponential function and a Mittag–Leffler function [26, 29]. Previous work in this field shows the approach is successful for parabolic partial differential equations [23, 34, 24]. Now we apply the approach to special matrices from chemistry [10, 41, 20].

2   A bimolecular master equation

Bimolecular reactions [3, 5, 35] between two chemical species S_1 and S_2 to form a third species S_3,

$$S_1 + S_2 \rightleftharpoons S_3 \,, \tag{4}$$

are now studied at single molecule resolution. A popular mathematical model is a continuous time Markov process, known as a chemical master equation, where states record the number of molecules of each species [10, 41, 20, 16, 11, 1, 6]. A state is (n_1, n_2, n_3) when there are n_1, n_2 and n_3 molecules of species S_1, S_2 and S_3, respectively. The probability p_i of state i is recorded in the ith element of the vector $\boldsymbol{p}$. These probabilities evolve according to the system of linear differential equations

$$\frac{d}{dt}\boldsymbol{p} = A\boldsymbol{p} \quad \text{with solution} \quad \boldsymbol{p}(t) = e^{At}\boldsymbol{p}(0) \,. \tag{5}$$

According to this master equation, the probability of transitioning from state j to state i in time dt is approximately given by the corresponding nonnegative off-diagonal entry: $A_{ij}dt$. Diagonal entries of A ensure zero column sum.

All our examples start in the initial state $(n_1, n_2, n_3) = (M - 1, M - 1, 0)$. State i is $(M-i, M-i, i-1)$ for $i = 1, \ldots M$. In our example (4), the forward reaction $(S_1 + S_2 \to S_3)$ rate is $c_f n_1 n_2$, and the backward rate is $c_b n_3$. Here c_f and c_b are rate constants that depend on chemical and physical properties. In this example, $A_{i+1,i} = c_f(M - i)^2$ and $A_{i,i+1} = c_b i$. This gives rise to a family of $M \times M$ tridiagonal matrices. With $c_f = c_b = 1$, the superdiagonal is $1, 2, \ldots, M - 1$ and the subdiagonal is $(M - 1)^2, (M - 2)^2, \ldots, 1^2$. A small example $(M = 6)$ is

$$
A = \begin{bmatrix}
-25 & 1 & & & & \\
25 & -17 & 2 & & & \\
& 16 & -11 & 3 & & \\
& & 9 & -7 & 4 & \\
& & & 4 & -5 & 5 \\
& & & & 1 & -5
\end{bmatrix}. \tag{6}
$$

All our figures use $M = 101$ and $c_b = 1$. Figures 2, 3 and 4 set $c_f = 1$. Figures 5, 6 and 7 set $c_f = 0.02$. The matrix exponential solution (5) is computed as $f(At)$, with $f(zt) = e^{zt}$, by the approximation (3) to the Cauchy integral (2).

Trapezoidal rules such as in (3) generically exhibit low rates of convergence but in the special case of periodic integrands, the rate of convergence is spectacular [40, 38], and the error in (3) decreases exponentially with N [43]. With only $N = 2^4$, quadrature points in Figure 1 (just eight are needed in our cases of real solutions when symmetry is exploited) we get excellent accuracy at $t = 1$ (Figure 2, bottom); using Matlab's `expm` as a reference solution, the maximum error across all components is $\approx 10^{-7}$.

However, at other t values the numerical method produces large errors. For example, at $t = 0.01$, Figure 2 (top) shows negative numbers that are

Figure 2: Numerical solution of bimolecular master equation (5) via the quadrature approximation (3) to the Cauchy integral (2). When $t = 0.01$ the approximation leads to significant error (top). When $t = 1$ the approximation is an accurate solution (bottom).
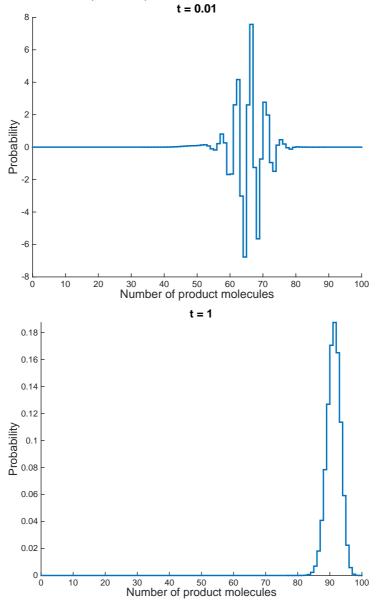
Figure 3: Resolvent norm of At on the parabolic contour Γ (1) (Figure 1) as computed by Chebfun [7]. This resolvent norm is very large when $t = 0.01$ (top), whereas the norm is approximately one when $t = 1$ (bottom).
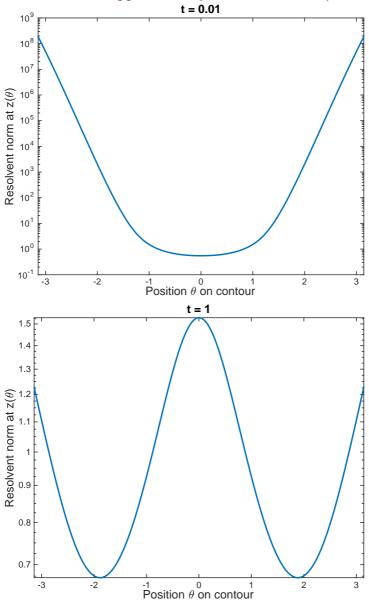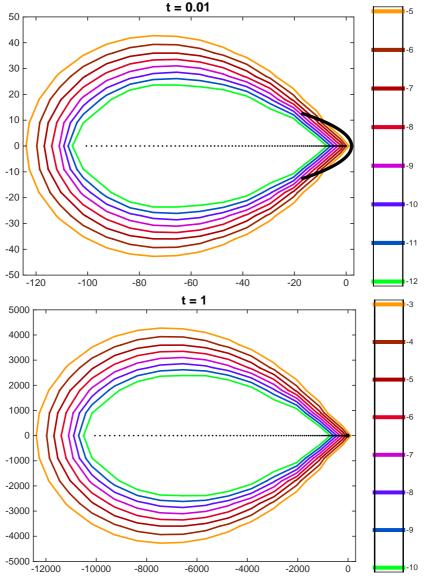
Figure 4: Level curves of the resolvent norm of At (6) as computed by EigTool [44] (minimum singular value $s_{min}(zI - At)$ shown on log scale). Eigenvalues are marked on the negative real axis. The parabolic contour Γ (Figure 1) is visible when $t = 0.01$ (top) but not when $t = 1$ (bottom).

impossible in the true solution, which is always a nonnegative probability vector. To understand the cause of the error it is instructive to examine the norm of the resolvent on the contour (Figure 3, as computed by Chebfun [7]). It is mild, $\mathcal{O}(1)$, at $t = 1$ but enormous, $\mathcal{O}(10^8)$, at $t = 0.01$. Although the overall error[1] comes from various sources [43, 42], Figure 4 suggests one source of error could be reduced by *choosing a wider contour* (such as a hyperbola) to avoid regions, known as the *pseudospectra*, where the resolvent is large [39]. For $\epsilon > 0$, the ϵ-pseudospectra is the region where $\|(zI - A)^{-1}\| > 1/\epsilon$ or, equivelently in the 2-norm, where the *minimum singular value* $s_{\min}$ is small:

$$\sigma_\epsilon \equiv \{z \in \mathbb{C} : s_{\min}(zI - A) < \epsilon\}.$$

Continuum approximations of master equations are related to convection-diffusion equations. For example, Gillespie [10] points out that a natural finite difference approximation to a Fokker–Planck equation recovers exactly a master equation. Such convection-diffusion like equations are known to have numerical issues associated with pseudospectra [31, 42, 15, 39] so it is likely that chemical master equations also have pseudospectra of numerical significance. EigTool [44] confirms this for the bimolecular example (6) in Figure 4. Top ($t = 0.01$) and bottom ($t = 1$) plots are nearly identical because the pseudospectra of At is a scaled version of the pseudospectra of A (real axis, imaginary axis and $s_{\min}$ are all multiplied by t).

Estimates of the pseudospectra, such as Figure 4, are desirable because they guide the choice of computationally preferable contours in (2). The same arguments of Reddy and Trefethen [31, Section 5] and of Trefethen and Embree [39, Section 12] applied to A in (6) lead to a bound[2]

$$\|(zI - A)^{-1}\| \leqslant \frac{\kappa}{|\operatorname{Im}(z)|}.$$

---

[1]This is not entirely fair to the method; the contour should allow dependence on t. Moreover, the method was designed with self-adjoint problems (unlike A) in mind.

[2]Here κ is the condition number of a matrix that symmetrizes A. For fixed M, this bound confines the pseudospectra to a strip of finite width about the real axis but unfortunately κ grows extremely fast with M.

Future work will explore finer estimates and connections of master equation matrices (6) to twisted Toeplitz matrices [39]. One encouraging aspect of Figure 4 is that the resolvent is largest in the far left plane, where numerical evaluation on the contour is not usually required. Notice for example that our contour (Figure 1) is not visible at the larger scales on the bottom plot of Figure 4.

3 Application to a fractional master equation

Often motivated from the viewpoint of continuous-time random walks, there has been much recent interest in fractional models and associated numerical methods [27, 18, 25, 12, 45, 2, 19, 30]. Using the Caputo fractional derivative

$$D_t^\alpha f(t) = \frac{1}{\Gamma(1-\alpha)} \int_0^t \frac{f'(s)}{(t-s)^\alpha} ds \,,$$

for $0 < \alpha \leqslant 1$ a time-fractional generalisation of the master equation (5) is

$$D_t^\alpha \mathbf{p} = A\mathbf{p} \quad \text{with solution} \quad \mathbf{p}(t) = E_\alpha(At^\alpha)\mathbf{p}(0)\,, \tag{7}$$

where E_α is the one-parameter Mittag–Leffler function

$$E_\alpha(z) = \sum_{k=0}^\infty \frac{z^k}{\Gamma(\alpha k + 1)}\,.$$

The exponential is recovered at $\alpha = 1$. The defining Markov features of A ensure columns of e^{At} are probability vectors. An intuitive way to to see that $E_\alpha(At^\alpha)$ shares this property with the exponential is via a representation of the Mittag–Leffler function as a mixture of exponentials, $E_\alpha(-t) = \int_0^\infty g(s)e^{-st}ds$, where $g(s)$ is a nonnegative probability density. When computing $E_\alpha(At^\alpha)$ as $f(At^\alpha)$ via (2) and (3), the linear solutions are now related to $(z^\alpha I - At^\alpha)^{-1}$ [43]. Numerical solutions via (3) for the usual exponential function ($\alpha = 1$) and for the Mittag–Leffler function ($\alpha = 0.6$)

are compared in Figures 5 and 6. Unlike for the exponential (Figure 3, top), $\|(z^\alpha I - At^\alpha)^{-1}\| \approx \mathcal{O}(1)$ is mild on Γ (we are also seeing the resolvent on the wider contour Γ^α for $\alpha = 0.6$), suggesting Mittag–Leffler evaluation is less sensitive to nonnormality for this example.

At very short timescales the reaction proceeds more quickly in the fractional model than in the more standard model that is not fractional (Figure 5, top), but at longer timescales the reaction proceeds more slowly in the fractional model (Figure 5, bottom). As $t \to \infty$, Figure 6 shows both the standard model (5) and the fractional model (7) tend to the same stationary distribution $\mathbf{p}_\infty$. This is understood by letting $A = V\Lambda V^{-1}$ be the eigenvalue decomposition and comparing solutions as matrix functions via diagonalization: $f(At^\alpha) = Vf(\Lambda t^\alpha)V^{-1}$, with $f(\lambda_j t^\alpha) = E_\alpha(\lambda_j t^\alpha)$. Eigenvalues λ_j of A, in the diagonal matrix Λ, are all negative except for a unique zero eigenvalue. For both the exponential function and the Mittag–Leffler function, $E_\alpha(0) = 1$ for $0 < \alpha \leqslant 1$, so the column of the eigenvector matrix V corresponding to the zero eigenvalue, which is the stationary distribution $\mathbf{p}_\infty$, persists as $t \to \infty$. All other eigenmodes decay because for $0 < \alpha \leqslant 1$ and $\lambda < 0$, $E_\alpha(\lambda t^\alpha) \to 0$ as $t \to \infty$. The rate of decay is always exponential ($\approx e^{-t}$) for $\alpha = 1$. However, when $0 < \alpha < 1$ asymptotics of the Mittag–Leffler function $E_\alpha(-t^\alpha)$ exhibit faster than exponential decay ($\approx e^{-t^\alpha}$) for $t \ll 1$, and much slower decay ($\approx 1/t^\alpha$) for large t. These are the familiar scalings of the Mittag–Leffler function, which behaves like a stretched exponential for small times and like an inverse power law for large times.

Monte Carlo simulation of fractional models by Gillespie-like algorithms [10] is possible by drawing from Mittag–Leffler waiting times, instead of from the usual exponential waiting times of a Markov process [14, 9, 33, 22]. A comparison of sample paths (Figure 7) reveals longer pauses in the fractional model associated with the heavy-tailed Mittag–Leffler waiting times. With 10^5 samples, Monte Carlo estimates of the distribution are in good agreement (Figure 5 and 6) with solutions of (7) but slow for these examples: a modern computer takes < 1 second to solve the fractional master equation in (7), or five minutes for 10^5 simulations.

Figure 5: A fractional generalisation of a bimolecular master equation has solution in terms of a Mittag–Leffler function (7), which is compared here to the exponential solution of the usual master equation (5).
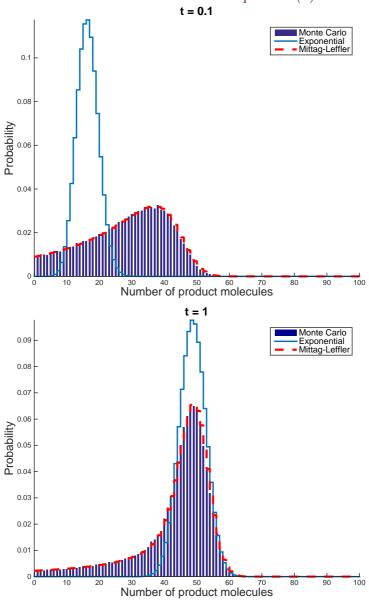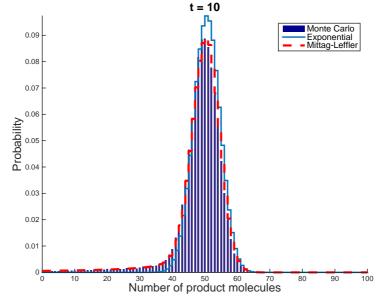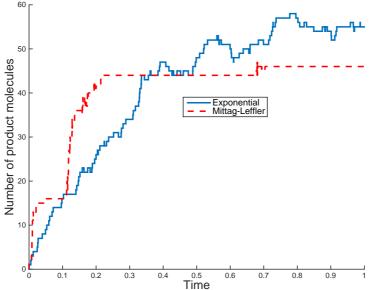
Figure 6: A fractional generalisation of a bimolecular master equation has solution in terms of a Mittag–Leffler function (7), which is compared here to the exponential solution of the usual master equation (5).

4   Discussion

A number of areas are now identified for further research, including: stochastic subordination [21], more flexible physical models [12], exploration of the pseudospectra in the 1-norm and ∞-norm [39], and the Toeplitz plus Hankel structures of fractional graph Laplacians or of fractional wave equations [36]. Finally, master equations in biology can involve high-dimensional problems in which matrices become so large that computing exponentials is not possible. Future work will extend the approaches here to larger scales by exploiting the parallelism that the Cauchy integral offers—the shifted linear systems $(z_k I - A)u_k = v$ of (3) may be solved independently and via iterative methods such as Krylov methods [28].

Figure 7: Two Monte Carlo simulations: one with exponential waiting times, and another with Mittag–Leffler waiting times. Histograms of many sample paths with Mittag–Leffler waiting times appear in Figures 5 and 6.

Conclusion   Cauchy integrals are effective in computationally solving bimolecular master equations. A benefit of the approach is that it offers a framework for fractional generalisations of master equations. However, chemical master equations involve nonnormal matrices for which the resolvent is large in significant regions of the complex plane; progress with the Cauchy integral approach requires further study of the pseudospectra. In contrast, stochastic simulation of sample paths via Gillespie-like approaches remains possible even in the presence of nonnormality.

References

[1] A. Andreychenko, L. Mikeev, D. Spieler, and V. Wolf. Approximate maximum likelihood estimation for stochastic chemical kinetics. *EURASIP J. Bioinf. Sys. Biol.*, 2012:9, 2012. doi:10.1186/1687-4153-2012-9 C35

[2] C. N. Angstmann, I. C. Donnelly, B. I. Henry, and J. A. Nichols. A discrete time random walk model for anomalous diffusion. *J. Comput. Phys.*, 293:53–69, 2014. doi:10.1016/j.jcp.2014.08.003 C41

[3] Y. Berkowitz, Y. Edery, H. Scher, and B. Berkowitz. Fickian and non-Fickian diffusion with bimolecular reactions. *Phys. Rev. E*, 87:032812, 2013. doi:10.1103/PhysRevE.87.032812 C35

[4] J. C. Butcher. On the numerical inversion of Laplace and Mellin transforms. *Conference on Data Processing and Automatic Computing Machines*, 117:1–8, 1957. C34

[5] D. Ding, D. A. Benson, A. Paster, and D. Bolster. Modeling bimolecular reactions and transport in porous media via particle tracking. *Adv. Water Resour.*, 53:56–65, 2013. doi:10.1016/j.advwatres.2012.11.001 C35

[6] B. Drawert, S. Engblom, and A. Hellander. URDME: a modular framework for stochastic simulation of reaction-transport processes in complex geometries. *BMC Syst. Biol.*, 6:76, 2012. doi:10.1186/1752-0509-6-76 C35

[7] T. A Driscoll, N. Hale, and L. N. Trefethen. *Chebfun Guide*. Pafnuty Publications, 2014. http://www.chebfun.org/docs/guide/ C38, C40

[8] N. Dunford and J. Schwartz. *Linear Operators I, II, III*. Wiley New York, 1971. http://au.wiley.com/WileyCDA/WileyTitle/productCd-0471608483.html, http://au.wiley.com/WileyCDA/WileyTitle/productCd-0471608475.html, http://au.wiley.com/WileyCDA/WileyTitle/productCd-0471608467.html C34

[9] D. Fulger, E. Scalas, and G. Germano. Monte Carlo simulation of uncoupled continuous-time random walks yielding a stochastic solution of the space-time fractional diffusion equation. *Phys. Rev. E*, 77:021122, 2008. doi:10.1103/PhysRevE.77.021122 C42

[10] D. Gillespie. *Markov Processes: An Introduction for Physical Scientists*. Academic Press, 1991. http://www.elsevier.com/books/markov-processes/gillespie/978-0-12-283955-9 C35, C40, C42

[11] M. Hegland, C. Burden, L. Santoso, S. MacNamara, and H. Booth. A solver for the stochastic master equation applied to gene regulatory networks. *J. Comput. Appl. Math.*, 205(2):708–724, 2006. doi:10.1016/j.cam.2006.02.053 C35

[12] B. I. Henry, T. A. M. Langlands, and S. L. Wearne. Anomalous diffusion with linear reaction dynamics: From continuous time random walks to fractional reaction-diffusion equations. *Phys. Rev. E*, 74(3):031116, 2006. doi:10.1103/PhysRevE.74.031116 C41, C44

[13] N. J. Higham. *Functions of Matrices*. SIAM, 2008. doi:10.1137/1.9780898717778 C34

[14] R. Hilfer and L. Anton. Fractional master equations and fractal time random walks. *Phys. Rev. E*, 51:R848, 1995. doi:10.1103/PhysRevE.51.R848 C42

[15] K. J. in 't Hout and J. A. C. Weideman. A contour integral method for the Black–Scholes and Heston equations. *SIAM J. Sci. Comput.*, 33:763–785, 2011. doi:10.1137/090776081 C40

[16] T. Jahnke and D. Altintan. Efficient simulation of discrete stochastic reaction systems with a splitting method. *BIT*, 50:797–822, 2010. doi:doi:10.1007/s10543-010-0286-0 C35

[17] T. Kato. *Perturbation theory for linear operators*. Springer-Verlag, 1976. http://link.springer.com/book/10.1007%2F978-3-642-66282-9 C34

[18] V. M. Kenkre, E. W. Montroll, and M. F. Shlesinger. Generalized master equations for continuous-time random walks. *J. Stat. Phys.*, 9(1):45, 1973. doi:10.1007/BF01016796 C41

[19] M. López-Fernández and C. Palencia. On the numerical inversion of the Laplace transform in certain holomorphic mappings. *Appl. Numer. Math.*, 51:289–303, 2004. doi:10.1016/j.apnum.2004.06.015 C41

[20] S. MacNamara, K. Burrage, and R. B. Sidje. Multiscale modeling of chemical kinetics via the master equation. *SIAM Multiscale Model. Simul.*, 6(4):1146–1168, 2008. doi:10.1137/060678154 C35

[21] M. Magdziarz, A. Weron, and K. Weron. Fractional Fokker–Planck dynamics: Stochastic representation and computer simulation. *Phys. Rev. E*, 75:016708, 2007. doi:10.1103/PhysRevE.75.016708 C44

[22] F. Mainardi, R. Gorenflo, and A. Vivoli. Beyond the Poisson renewal process: A tutorial survey. *J. Comput. Appl. Math.*, 2007. doi:10.1016/j.cam.2006.04.060 C42

[23] W. McLean. Regularity of solutions to a time-fractional diffusion equation. *ANZIAM J.*, 52(2):123–138, 2010. doi:10.1017/S1446181111000617 C35

[24] W. McLean and V. Thomée. Time discretization of an evolution equation via Laplace transforms. *IMA J. Numer. Anal.*, 24:439–463, 2004. doi:10.1093/imanum/24.3.439 C35

[25] R. Metzler and J. Klafter. The random walk's guide to anomalous diffusion: a fractional dynamics approach. *Phys. Rep.*, 339:1–77, 2000. doi:10.1016/S0370-1573(00)00070-3 C41

[26] C. Moler and C. Van Loan. Nineteen Dubious Ways to Compute the Exponential of a Matrix, 25 Years Later. *SIAM Rev.*, 45(1):3–49, 2003. doi:10.1137/S00361445024180 C35

[27] E. W. Montroll and G. H. Weiss. Random Walks on Lattices. II. *J. Math. Phys.*, 6(2):167–181, 1965. doi:10.1063/1.1704269 C41

[28] I. Moret and P. Novati. On the Convergence of Krylov Subspace Methods for Matrix Mittag–Leffler Functions. *SIAM J. Numer. Anal.*, 49(5):2144–2164, 2011. doi:10.1137/080738374 C44

[29] I. Podlubny. *Fractional Differential Equations*. Academic Press, San Diego, 1999. http://www.elsevier.com/books/fractional-differential-equations/podlubny/978-0-12-558840-9 C35

[30] M. Raberto, F. Rapallo, and E. Scalas. Semi-Markov Graph Dynamics. *PLoS ONE*, 6(8):e23370, 2011. doi:10.1371/journal.pone.0023370 C41

[31] S. C. Reddy and L. N. Trefethen. Pseudospectra of the convection-diffusion operator. *SIAM J. Appl. Math.*, 54(6):1634–1649, 1994. doi:10.1137/S0036139993246982 C40

[32] E. B. Saff and A. D. Snider. *Fundamentals of complex analysis with applications to engineering and science*. Pearson Education, 2003. http://www.pearsonhighered.com/educator/product/Fundamentals-of-Complex-Analysis-with-Applications-to-Engineer9780139078743.page C33

[33] E. Scalas, R. Gorenflo, and F. Mainardi. Uncoupled continuous-time random walks: Solution and limiting behavior of the master equation. *Phys. Rev. E*, 69:011107, 2004. doi:10.1103/PhysRevE.69.011107 C42

[34] D. Sheen, I. H. Sloan, and V. Thomée. A parallel method for time discretization of parabolic equations based on Laplace transformation and quadrature. *IMA J. Numer. Anal.*, 23:269–299, 2003. doi:10.1093/imanum/23.2.269 C35

[35] M. J. Shon and A. E. Cohen. Mass action at the single-molecule level. *J. Am. Chem. Soc.*, 134(35):14618–14623, 2012. doi:10.1021/ja3062425 C35

[36] G. Strang and S. MacNamara. Functions of difference matrices are Toeplitz plus Hankel. *SIAM Rev.*, 56(3):525–546, 2014. doi:10.1137/120897572 C44

[37] A. Talbot. The accurate numerical inversion of Laplace transforms. *J. Inst. Math. Appl.*, 23:97–120, 1979. doi:10.1093/imamat/23.1.97 C34

[38] L. N. Trefethen. *Approximation Theory and Approximation Practice*. SIAM, Philadelphia, 2013. http://bookstore.siam.org/ot128/ C36

[39] L. N. Trefethen and M. Embree. *Spectra and pseudospectra: the behavior of nonnormal matrices and operators*. Princeton University Press, 2005. http://press.princeton.edu/titles/8113.html C40, C41, C44

[40] L. N. Trefethen and J. A. C. Weideman. The exponentially convergent trapezoidal rule. *SIAM Rev.*, 56(3):385–458, 2014. doi:10.1137/130932132 C34, C36

[41] N. G. van Kampen. *Stochastic Processes in Physics and Chemistry*. Elsevier Science, 2001. http://www.elsevier.com/books/stochastic-processes-in-physics-and-chemistry/van-kampen/978-0-444-52965-7 C35

[42] J. A. C. Weideman. Improved contour integral methods for parabolic PDEs. *IMA J. Numer. Anal.*, 30:334–350, 2010. doi:10.1093/imanum/drn074 C40

[43] J. A. C. Weideman and L. N. Trefethen. Parabolic and hyperbolic contours for computing the bromwich integral. *Math. Comput.*, 76:1341–1356, 2007. doi:10.1090/S0025-5718-07-01945-X C34, C35, C36, C40, C41

[44] T. G. Wright. Eigtool, 2002. http://www.comlab.ox.ac.uk/pseudospectra/eigtool/. C39, C40

[45] Q. Yang, T. Moroney, K. Burrage, I. Turner, and F. Liu. Novel numerical methods for time-space fractional reaction diffusion equations

in two dimensions. *ANZIAM J.*, 52:395–409, 2011. http://journal.austms.org.au/ojs/index.php/ANZIAMJ/article/view/3791/1463 C41

Author address

1. **S. MacNamara**, School of Mathematics and Statistics, University of New South Wales, Sydney, Australia.
   mailto:s.macnamara@unsw.edu.au